Applied Physics Express **4** (2011) 082104
DOI: 10.1143/APEX.4.082104

High-Power Blue-Violet Semipolar ($20\bar{2}\bar{1}$) InGaN/GaN Light-Emitting Diodes with Low Efficiency Droop at 200 A/cm^2

Yuji Zhao[1]*, Shinichi Tanaka[2], Chih-Chien Pan[2], Kenji Fujito[3], Daniel Feezell[2], James S. Speck[2], Steven P. DenBaars[1,2], and Shuji Nakamura[1,2]

[1] *Electrical and Computer Engineering Department, University of California, Santa Barbara, CA 93106, U.S.A.*
[2] *Materials Department, University of California, Santa Barbara, CA 93106, U.S.A.*
[3] *Optoelectronic Laboratory, Mitsubishi Chemical Corporation, Ushiku, Ibaraki 300-1295, Japan*

Received June 18, 2011; accepted June 30, 2011; published online July 15, 2011

We report a high-power blue light-emitting diode (LED) with a high external quantum efficiency and low droop on a free-standing ($20\bar{2}\bar{1}$) GaN substrate. At a forward current of 20 mA, the LED showed a peak external quantum efficiency of 52% and an output power of 30.6 mW. In higher current density regions, the LED also showed outstanding performance, with droop ratios of 0.7% at 35 A/cm^2, 4.3% at 50 A/cm^2, 8.5% at 100 A/cm^2, and 14.3% at 200 A/cm^2. The output power and external quantum efficiency at 200 A/cm^2 were 266.5 mW and 45.3%, respectively.

Light-emitting diodes (LEDs) based on InGaN technology enable a wide range of applications including traffic signals, full-color displays, backlighting sources for liquid-crystal displays, and general lighting.[1)] At present, the widespread adoption of LEDs, particularly for general lighting, requires cost reductions and improvements in device performance. One path toward lower cost is the reduction of the LED footprint and the operation of small-area (<0.1 mm^2) LEDs at high current densities (e.g., beyond 100 A/cm^2) for high-power applications. However, the realization of viable devices in this operating regime requires the elimination of the phenomenon known as "efficiency droop", which refers to the reduction in external quantum efficiency (EQE) observed at higher injection currents.[2)] The physical origin of efficiency droop is still being debated and several different mechanisms have been proposed as explanations, including carrier leakage,[2)] Auger recombination,[3,4)] carrier delocalization,[5)] defects,[6)] and junction heating.[7)]

Current commercially available InGaN-based LEDs grown on the "polar" *c*-plane of the crystal suffer from internal polarization-related electric fields that separate the electron and hole wave functions in the quantum wells and limit the radiative recombination rate.[8–11)] On the other hand, devices grown on nonpolar or semipolar orientations have been demonstrated with eliminated or reduced polarization fields[12–15)] and are theoretically predicted to have higher radiative recombination rates than *c*-plane devices.[16)] To date, high-efficiency semipolar blue[17)] and green LEDs[18)] have been demonstrated. Recently, semipolar planes such as the ($20\bar{2}1$) plane, which is miscut 15 degrees from the *m*-plane, have attracted significant interest due to their promising performance in the green region of the spectrum.[18–21)] In this work, we report for the first time a blue-violet InGaN/GaN LED on a free- standing semipolar ($20\bar{2}\bar{1}$) bulk GaN substrate with a high light output power, EQE greater than 50%, and low droop ratios of 0.7% at 35 A/cm^2, 4.3% at 50 A/cm^2, 8.5% at 100 A/cm^2, and 14.3% at 200 A/cm^2.

LED epitaxial layers were homoepitaxially grown by conventional metal organic chemical vapor deposition (MOCVD) on free-standing ($20\bar{2}\bar{1}$) GaN substrates supplied by Mitsubishi Chemical Corporation. The device structure consists of a 1 µm Si-doped n-type GaN layer, ten sets of Si-doped InGaN/GaN superlattices, three periods of InGaN (3 nm)/GaN (13 nm) multiple quantum wells (MQWs), a five-set Mg-doped AlGaN/GaN superlattice electron blocking layer (EBL), and a 60 nm p-type GaN layer. For the ($20\bar{2}\bar{1}$) LED fabrication, a rectangular mesa pattern (active area of 0.1 mm^2) was formed by conventional lithography and chlorine-based inductively coupled plasma (ICP) etching after an indium tin oxide (ITO) current-spreading layer was deposited by electron beam evaporation. Ti/Al/Ni/Au n-type contacts and Ti/Au pads were deposited by electron beam evaporation and a conventional lift-off process. To improve the light extraction efficiency, the backside of the LED was roughened[17)] and packaged with a vertical stand transparent structure.[22)] A schematic of the device with the roughened backside and a schematic view of the ($20\bar{2}\bar{1}$) plane in the wurtzite structure are presented in Figs. 1 and 2, respectively.

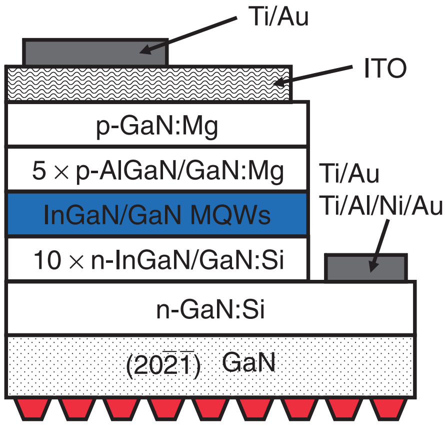

Fig. 1. Schematic view of the semipolar ($20\bar{2}\bar{1}$) LED device with backside roughening structures.

Room-temperature electroluminescence (EL) measurements under pulsed conditions with a duty cycle of 1% were performed in a calibrated integrating sphere. Figure 3 presents the light output power vs current density and EQE vs current density curves for the LED. At a forward current of 20 mA, the semipolar LED had an output power of 30.6 mW and an EQE of 52%, which are comparable to the

*E-mail address: yujizhao@engineering.ucsb.edu

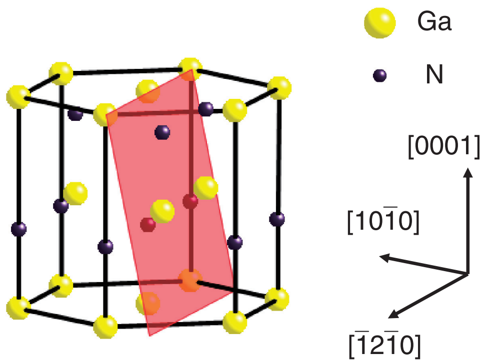

Fig. 2. Schematic view of semipolar $(20\bar{2}\bar{1})$ in the wurtzite crystal structure.

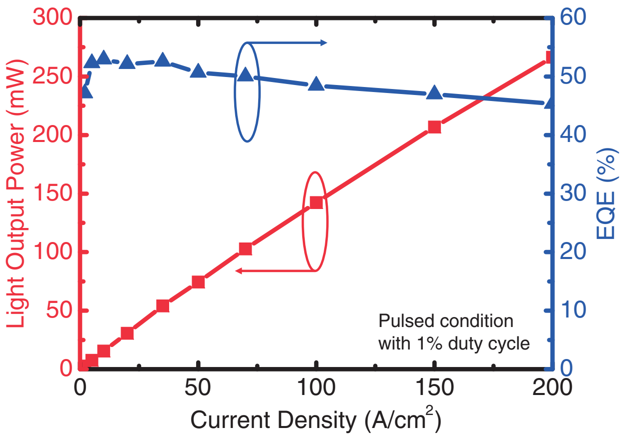

Fig. 3. Light output power vs current density and external quantum efficiency vs current density curves for a packaged $(20\bar{2}\bar{1})$ LED under pulsed operation.

Table I. EQE and droop performance of semipolar blue-violet $(20\bar{2}\bar{1})$ LED at various current densities.

	35 A/cm^2	50 A/cm^2	100 A/cm^2	200 A/cm^2
EQE (%)	52.6	50.7	48.4	45.3
Droop (%)	0.7	4.3	8.5	14.3

best values ever reported for semipolar or nonpolar LEDs.[17) Moreover, the LED device demonstrates outstanding droop performance at high current densities. Table I shows the EQE and efficiency droop of the LED at various current densities. The LED exhibits only 0.7% efficiency droop at a current density of 35 A/cm^2 and shows a low droop of 14.3% at a current density of 200 A/cm^2. The droop ratio was defined as droop ratio = $(\text{EQE}_{max} - \text{EQE}_{cd})/\text{EQE}_{max} \times 100\%$, where the EQE_{max} and EQE_{cd} represent the EQE maximum and the EQE at different current densities, respectively. To the best of the author's knowledge, such a low droop has not been reported at current densities of 200 A/cm^2.

Figure 4 shows the EL peak wavelength and full width at half maximum (FWHM) of the LED at different drive

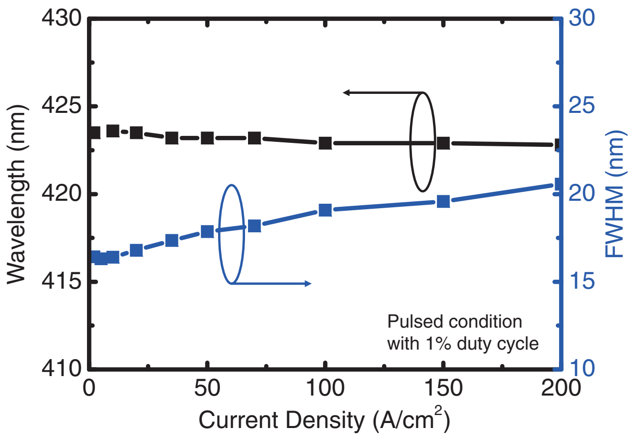

Fig. 4. EL peak wavelength and FWHM of the semipolar $(20\bar{2}\bar{1})$ LED at different current densities under pulsed operation.

currents under pulse operation. The LED shows a negligible wavelength shift up to 200 A/cm^2, indicating greatly reduced polarization-related electric fields inside the QWs. This result is also consistent with previously reported *m*-plane LEDs.[13) Moreover, the LED exhibits a very small FWHM in both low-and high-current-density regions, which suggests good compositional and structural uniformity for the InGaN QWs. The underlying cause of the low efficiency droop on semipolar $(20\bar{2}\bar{1})$ LEDs is a topic of ongoing investigation and will be reported elsewhere.

In summary, we have demonstrated a high-power blue-violet semipolar $(20\bar{2}\bar{1})$ LED with an EQE above 50% with low droop operating up to 200 A/cm^2. The droop ratios were 0.7% at 35 A/cm^2, 4.3% at 50 A/cm^2, 8.5% at 100 A/cm^2, and 14.3% at 200 A/cm^2. The development of devices with reduced droop at high current densities is ultimately desirable for cost savings and to expedite the adoption of LEDs for general lighting applications. The LED also shows a stable peak wavelength with increasing drive current and a narrow FWHM, indicating low polarization-related electric fields and compositionally uniform InGaN. These results suggest that specific semipolar orientations may provide benefits for droop reduction in high-power, small-area LEDs.

Acknowledgments The authors acknowledge the support of the Solid State Lighting and Energy Center at UCSB. A portion of this work was done at the UCSB nanofabrication facility, part of the National Science Foundation (NSF)-funded National Nanotechnology Infrastructure Network (NNIN).

1) S. Nakamura, T. Mukai, and M. Senoh: Appl. Phys. Lett. **64** (1994) 1687.
2) M. H. Kim, M. F. Schubert, Q. Dai, J. K. Kim, E. F. Schubert, J. Piprek, and Y. Park: Appl. Phys. Lett. **91** (2007) 183507.
3) Y. C. Shen, G. O. Müller, S. Watanabe, N. F. Gardner, A. Munkholm, and M. R. Krames: Appl. Phys. Lett. **91** (2007) 141101.
4) E. Kioupakis, P. Rinke, K. T. Delaney, and C. G. Van de Walle: Appl. Phys. Lett. **98** (2011) 161107.
5) S. F. Chichibu, T. Azuhata, M. Sugiyama, T. Kitamura, Y. Ishida, H. Okumura, H. Nakanishi, T. Sota, and T. Mukai: J. Vac. Sci. Technol. B **19** (2001) 2177.
6) B. Monemar and E. B. Sernelius: Appl. Phys. Lett. **91** (2007) 181103.
7) A. A. Efremov, N. I. Bochkareva, R. I. Gorbunov, D. A. Larinovich, Yu. T. Rebane, D. V. Tarkhin, and Yu. G. Shreter: Semiconductors **40** (2006) 605.
8) F. Bernardini and V. Fiorentini: Phys. Status Solidi B **216** (1999) 391.
9) A. Hangleiter, J. S. Im, H. Kollmer, S. Heppel, J. Off, and F. Scholz: MRS

Internet J. Nitride Semicond. Res. **3** (1998) 15.
10) A. E. Romanov, T. J. Baker, S. Nakamura, and J. S. Speck: J. Appl. Phys. **100** (2006) 023522.
11) S. Chichibu, T. Azuhata, T. Sota, and S. Nakamura: Appl. Phys. Lett. **69** (1996) 4188.
12) P. Walterweit, O. Brandt, A. Trampert, H. T. Grahn, J. Menniger, M. Ramsteiner, M. Reiche, and K. H. Ploog: Nature (London) **406** (2000) 865.
13) M. Schmidt, K. Kim, H. Sato, N. Fellows, H. Masui, S. Nakamura, S. P. DenBaars, and J. S. Speck: Jpn. J. Appl. Phys. **46** (2007) L126.
14) H. Zhong, A. Tyagi, N. Fellows, F. Wu, R. B. Chung, M. Saito, K. Fujito, J. S. Speck, S. P. DenBaars, and S. Nakamura: Appl. Phys. Lett. **90** (2007) 233504.
15) Y. Zhao, J. Sonoda, I. Koslow, C. C. Pan, H. Ohta, J. S. Ha, S. P. DenBaars, and S. Nakamura: Jpn. J. Appl. Phys. **49** (2010) 070206.
16) S. H. Park and D. Ahn: Appl. Phys. Lett. **90** (2007) 013505.
17) Y. Zhao, J. Sonoda, C. C. Pan, S. Brinkley, I. Koslow, K. Fujito, H. Ohta, S. P. DenBaars, and S. Nakamura: Appl. Phys. Express **3** (2010) 102101.
18) S. Yamamoto, Y. Zhao, C. C. Pan, R. B. Chung, K. Fujito, J. Sonoda, S. P. DenBaars, and S. Nakamura: Appl. Phys. Express **3** (2010) 122102.
19) Y. Enya, Y. Yoshizumi, T. Kyono, K. Akita, M. Ueno, M. Adachi, T. Sumitomo, S. Tokuyama, T. Ikegami, K. Katayama, and T. Nakamura: Appl. Phys. Express **2** (2009) 082101.
20) T. Kyono, Y. Yoshizumi, Y. Enya, M. Adachi, S. Tokuyama, M. Ueno, K. Katayama, and T. Nakamura: Appl. Phys. Express **3** (2010) 011003.
21) Y. D. Lin, S. Yamamoto, C. Y. Huang, C. L. Hsiung, F. Wu, K. Fujito, H. Ohta, J. S. Speck, S. P. DenBaars, and S. Nakamura: Appl. Phys. Express **3** (2010) 082001.
22) C. C. Pan, I. Koslow, J. Sonoda, H. Ohta, J. S. Ha, S. Nakamura, and S. P. DenBaars: Jpn. J. Appl. Phys. **49** (2010) 080210.